Environment International 182 (2023) 108282

Contents lists available at ScienceDirect

Environment International

journal homepage: www.elsevier.com/locate/envint

Full length article

What is hiding below the surface – MPs including TWP in an urban lake

Marziye (Shabnam) Molazadeh *, Fan Liu, Jeanette Lykkemark, Lucian lordachescu, Asbjørn Haaning Nielsen, Jes Vollertsen

Aalborg University, Section of Civil and Environmental Engineering, Department of the Built Environment, Thomas Manns Vej 23, 9220 Aalborg Øst, Denmark

ARTICLE INFO

Handling Editor: Adrian Covaci

Keywords:
Urban Lake
Sediments
Microplastics
Tyre wear particles
μFTIR
Py-GC/MS

ABSTRACT

Inland lakes play an important role as habitats for local species and are often essential drinking water reservoirs. However, there is limited information about the presence of microplastics (MPs) in these water bodies. Thirteen sediment samples were collected across a Danish urban lake to map MPs, including tyre wear particles (TWP). The lower size detection limit was 10 μm. MPs were quantified as counts, size, and polymer type by Fourier-transform infrared microspectroscopy (μFTIR) and mass estimated from the 2D projections of the MPs. As TWP cannot be determined by μFTIR, counts and sizes could not be quantified by this technique. Instead, TWP mass was determined by pyrolysis gas chromatography mass spectrometry (Py-GC/MS). The average MP abundance was 279 mg kg^{-1} (μFTIR), of which 19 mg kg^{-1} (Py-GC/MS) were TWP. For MPs other than tyre wear, the average MP count concentration was 11,312 counts kg^{-1}. Urban runoff from combined sewer overflows and separate stormwater outlets combined with outflow from a wastewater treatment plant were potential point sources. The spatial variation was substantial, with concentrations varying several orders of magnitude. There was no pattern in concentration across the lake, and the distribution of high and low values seemed random. This indicates that large sampling campaigns encompassing the entire lake are key to an accurate quantification. No preferential spatial trend in polymer characteristics was identified. For MPs other than TWP, the size of buoyant and non-buoyant polymers showed no significant difference across the lake, suggesting that the same processes brought them to the sediment, regardless of their density. Moreover, MP abundance was not correlated to sediment properties, further indicating a random occurrence of MPs in the lake sediments. These findings shed light on the occurrence and distribution of MPs, including TWP, in an inland lake, improving the basis for making mitigation decisions.

1. Introduction

Plastic is versatile, resilient, cheap, and lightweight. These properties have led to its ever-growing use, with manufacture currently reaching approximately 300 million tons worldwide in the last 50 years (Bharath et al., 2021). Upon use, most plastic is landfilled or burned, while some is simply dumped in the environment (Yang et al., 2022). Only about 9 % of plastic waste is recycled globally, leading to significant stress on the environment and natural resources (OECD, 2023).

Once MPs are in the environment, they tend to persist. Their breakdown into smaller MPs, chemical degradation, and biological decomposition is slow and strongly dependent on the environment they are in (Corcoran, 2020). Where there is no light and little oxidative potential, they may persist for generations (Simon-Sánchez et al., 2022). MPs are found all over the globe, from the high artic (Gündoğdu et al., 2021) to the world's desserts (Wang et al., 2021). The spreading is facilitated by their small size and low density, leading to them being easily spread and transported by wind and water over long distances (Reimonn et al., 2019). MPs are present in habitats worldwide, from soil to water and atmosphere (Molazadeh et al., 2022; Simon-Sánchez et al., 2022; Vianello et al., 2019), even in habitats of sparsely populated regions, such as Antarctica (Kelly et al., 2020).

Plastics are suspected to cause physical harm to organisms such as fish, mammals, invertebrates, and birds upon intake (Cole et al., 2015; Lusher et al., 2016; Monclús et al., 2022). Small MPs and nanoplastics (NP) might also translocate into the tissue of organisms, causing detrimental impacts (Dong et al., 2023). Finally, some MPs may act as vectors for toxic compounds, either by sorbing pollutants from the environment or by containing toxic additives (Besseling et al., 2019; Cole et al., 2011). An example of the latter is tyre wear particles (TWP), a MP type

* Corresponding author.
E-mail address: marziyem@build.aau.dk (M.(S. Molazadeh).

https://doi.org/10.1016/j.envint.2023.108282
Received 26 July 2023; Received in revised form 14 October 2023; Accepted 20 October 2023
Available online 31 October 2023

which lately has been identified as a potentially rather toxic part of the microplastic litter (Knight et al., 2020).

MPs in freshwaters have in recent years received increasing attention, partly because freshwaters can convey MPs to the marine environment, and partly because MPs may affect their ecosystems. Inland lakes are, in this respect, of considerable importance as they provide habitats for local species and often act as drinking water reservoirs (Eriksen et al., 2013; Islam et al., 2022). Some of these are urban lakes which receive urban and highway runoff, resulting in them receiving more anthropogenic pollutants, e.g., MPs, than many natural lakes (Hengstmann et al., 2021).

The level of MP pollution in lakes has been shown to be comparable to that of marine waters (Ding et al., 2019; Yonkos et al., 2014). Moreover, inland lakes, especially in densely populated urban areas, are typically much smaller than the open sea, which leads to less dilution and hence potentially higher concentration and accumulation in their sediments. While the presence of MPs in lakes has been reported by several studies (Mercy et al., 2023; Scopetani et al., 2019; Srinivasalu et al., 2021; Malla-Pradhan et al., 2022), their occurrence and distribution in urban lakes is less well documented, and data on TWP is scarce. The objective of the present study is to add knowledge on MP including TWP in such lakes by studying their occurrence in the sediments and analysing their spatial variability within a lake. The MPs are quantified by Fourier-transform infrared microspectroscopy (μFTIR imaging) and by pyrolysis gas chromatography mass spectrometry (Py-GC/MS) for TWP.

2. Material and methods

2.1. Site description and sample collection

Brabrand Lake (Brabrand Sø) is in the western part of Aarhus city, Denmark, and is surrounded by a dense littoral zone with reeds and wet meadows (Matamoros et al., 2012). It receives water from Aarhus River (Århus Å) after it has passed the artificial wetland Århus Engsø (56°144706 N, 10°096916 E) established in 1998. It discharges to the lower part of Aarhus River at Andebroen (56°140339 N, 10°144498 E), which ultimately discharges to the Aarhus Bay in the centre of the city. The lake furthermore receives urban runoff from numerous separate stormwater outlets and combined sewer overflows, as well as discharge from a wastewater treatment plant (WWTP) (Viby Renseanlæg) via Døde Å (Dead River) (56°137945, 10°136352). The treatment plant serves pprox.. 120,000 population equivalents and applies mechanical pre-treatment, nitrification, denitrification, phosphorous removal, and a final polishing of the effluent through a sand filter. The lake covers 153.8 ha and has a total catchment of 31,000 ha. The average water depth is 0.85 m, and the maximum is 2.70 m (Fig. 1). Moreover, the water in the lake has an average hydraulic retention time of 12 days. The full extent of the lake was dredged in 1988–1995, where 0.5 million m^3 of sediment was removed to a depth between 0 and 0.9 m. Legacy pollution from before the establishment of the wastewater treatment plant was hereby removed.

To assess the amount of MPs including TWP accumulated in the lake sediments, five transects were laid out at which a total of 13 samples were collected (Fig. 1). A Van Veen grab was used for the sampling, which was conducted in August 2021. The sediment was sampled in a

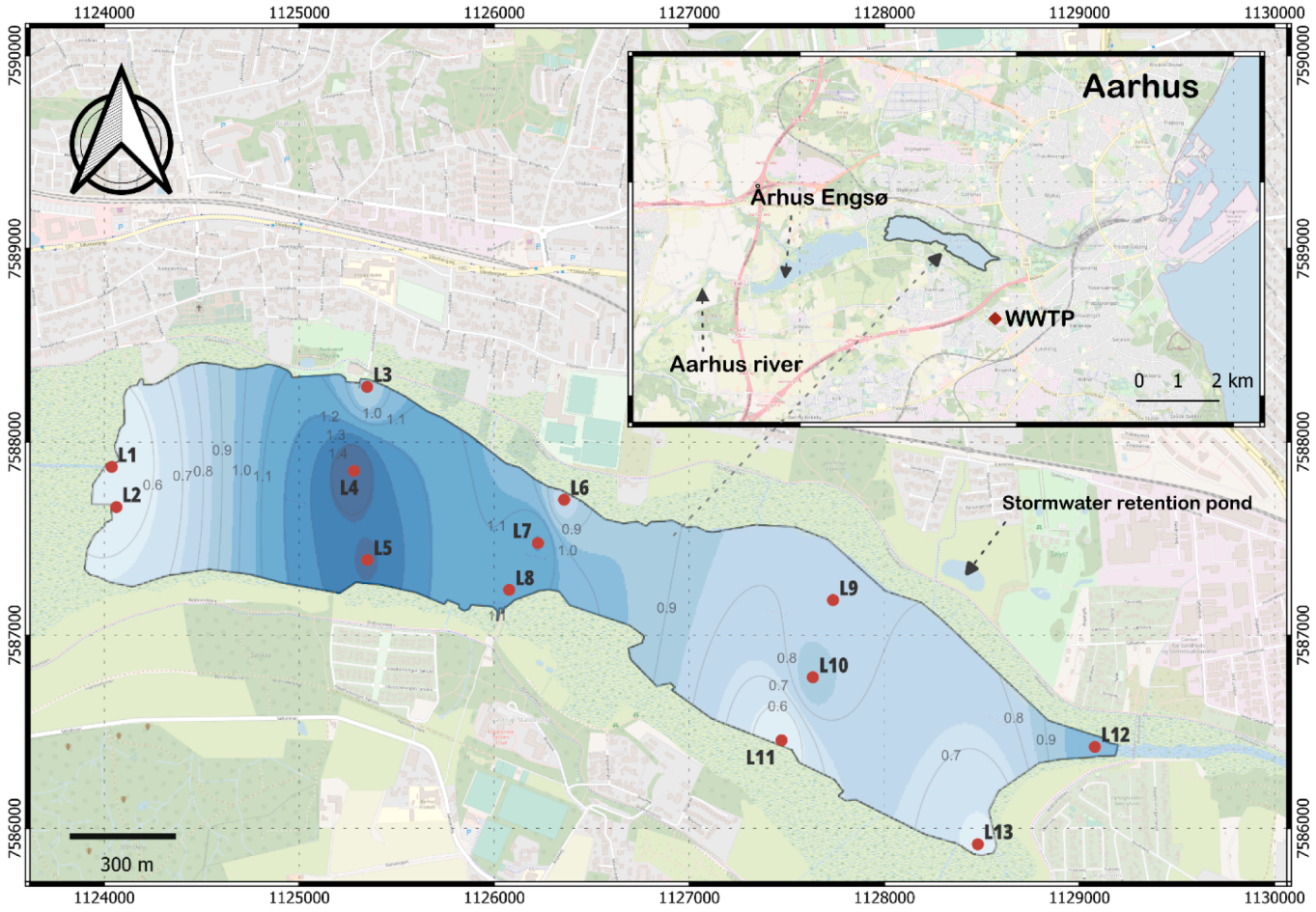

Fig. 1. Map of the lake showing the sampling stations (L1–L13). The inlet is in the western part of the lake, while the outlet is in its eastern part.

dry period, defined as no rain at least 2 days prior to the activity. For each sampling location, 2–3 kg of bulk sediment from the top 5–8 cm of each grab was collected and stored in a glass jar. The lake has an annual sediment accumulation rate of about 1 cm per year (Søndergaard et al., 2008). Thus, the samples are expected to represent recent sediment deposition covering about 5–8 years. The samples were immediately transferred to the laboratory and stored at 5 °C for further analysis.

2.2. Sediment characteristics

Sediments were characterised for organic matter content and grain size distribution. The former was done by muffling dried sediment of known weight at 550 °C for 4 h in a muffle furnace, and the weight loss on ignition was determined (ASTM, 2000). The grain size distribution followed the same procedure as described by Molazdeh et al. (2023). In brief, sieves with different mesh sizes were used for size classification of grains > 63 μm and hydrometer tests were used for grains < 63 μm (Asadi et al., 2019).

2.3. MP extraction

MPs were isolated by following the procedure described by Molazdeh et al. (2023). In brief, approximately 1.5 kg of homogenised subsample was taken from the jar and transferred into a pre-cleaned glass beaker. The subsample was pre-oxidised by gradually adding hydrogen peroxide (50 % H_2O_2) and Milli-Q water while gently stirring the sediment to achieve a maximum of 10 % H_2O_2 as the final concentration. The process was repeated until no foaming occurred when adding H_2O_2. The oxidised samples were wet sieved through 2 mm and 5 mm stainless steel sieves (Retsch GmbH, Germany) before drying in an oven at 50 °C until a constant dry weight was achieved. Of the < 2 mm dried samples, subsamples of 100 g went through density separation using sodium polytungstate (SPT) solution ($\rho = 1.8$ g cm^{-3}) in a 2 L pear-shaped separator funnel.

The mixture of sediment and SPT in the funnel was aerated for 30 min by passing filtered compressed air from the bottom, then left to settle for 24 h, upon which the settled fraction was drained away while the floating fraction was filtered through a 10 μm stainless steel filter. The collected particles were then transferred into a sodium dodecyl sulphate (SDS, 5 % w/vol) solution with a constant stirring and incubated at 50 °C for 48 h. To further degrade the remaining organic material, the particles underwent a two-step enzymatic digestion using a blend of cellulase (Cellulase enzyme blend®, Sigma-Aldrich) and cellulolytic enzymes (Viscozyme®L, Sigma-Aldrich) for 48 h, followed by protease, for another 48 h (Protease from Bacillus sp.®, Sigma-Aldrich) (Chand et al., 2022; Molazadeh et al., 2023). Both steps were performed at 50 °C. Subsequently, the samples underwent a Fenton oxidation by transferring the filtered particles into 200 mL of Milli-Q water, with the addition of 145 mL 50 % H_2O_2 and 62 mL of 0.1 M iron sulphate ($FeSO_4$). The pH of the mixture was adjusted to 3 by adding 65 mL of 0.1 M sodium hydroxide (NaOH) while the temperature was maintained at 15–30 °C. The collected particles were split into two size fractions by filtering over a 10 μm and a 500 μm stainless steel mesh. The large particles retained on the larger mesh were collected and dried at 55 °C, after which they were added to the fraction of 2–5 mm and analysed one by one. Particles < 500 μm were transferred to a 250 mL separation funnel with SPT solution ($\rho = 1.8$ g cm^{-3}), and went through a second density separation following the same procedure as described previously. The floating particles were filtered through a 10 μm stainless filter and transferred into 50 % ethanol (HPLC grade), upon which they were transferred to a 10 mL glass vial and dried in an automated solvent evaporator (TurboVap® LV, Biotage) at 50 °C. Finally, 5 mL 50 % ethanol was added to the vial to mobilise the particles.

2.4. MP and TWP analysis

2.4.1. Particles > 500 μm

Potential MPs > 500 μm were visually sorted and photographed under a stereomicroscope (ZEISS, SteREO Discovery.V8, Oberkochen Germany). The software ZenCore (Zen2Core SP1 from ZEISS) was used to measure their morphology. All suspicious particles were then analysed by Attenuated total reflectance (ATR) FTIR spectrometry (Cary 630 Agilent Technologies, with a single reflection diamond ATR) for chemical composition. The obtained IR spectra were compared with a commercial library in the software OMNIC (Thermo Fisher Scientific Inc., 8.2.0.387 version 1). If particles suspected to contain TWP had been seen, these would have been analysed by Py-GC/MS. The particle mass was estimated from the area of the particle images applying the same approach as for the MP < 500 μm.

2.4.2. Particles < 500 μm

2.4.2.1. MP analysis. After homogenising the 5 mL solution well, an aliquot was deposited on a Ø13 × 2 mm circular zinc selenide window using a glass capillary micropipette. The window was restricted by a compression cell with a Ø10 mm effective area (Pike Technologies). The window with its deposited aliquot was dried on a heating plate at 55 °C. This procedure was repeated until enough particles were deposited on the window. For each sample, the deposition was done for at least three windows to ensure that the deposited volume was representative of the whole sample. After drying, the window was scanned employing focal plane array (FPA) μFTIR imaging (Agilent Cary 620 FTIR microscope equipped with a 128 × 128 pixel FPA Mercury Cadmium Telluride detector, coupled with an Agilent 670 IR spectroscope), resulting in a pixel resolution of 5.5 μm. The acquired IR map was analysed by siMPle, a freeware for automated MP detection (Primpke et al., 2020b). The software allows detection of MP polymer type, size, and shape of particles, and estimates their mass based here on. The library used for this study was based on the library used by Rist et al. (2020), but extended to 380 reference spectra, covering both synthetic and natural materials (Molazade et al., 2023).

2.4.2.2. TWP analysis. Py-GC/MS was used to measure the concentration of TWP in the sediment extracts. An aliquot of 50–750 μL from the 5 mL concentrates was added to a sample cup using a glass capillary micropipette and dried on a heating plate at 30 °C. The Py-GC/MS consisted of a microfurnace pyrolyzer EGA/Py-3030D (FrontierLab, Japan) and an auto-shot sampler AS-1020E (FrontierLab, Japan) unit connected to a Thermo Scientific TRACE 1310 GC and an ISQ™ single quadrupole GC/MS part, using helium as the carrier gas. The gas from the pyrolyzer was injected in split mode (ratio 30:1). Deuterated polystyrene (PS-d8, 0.2 g/L) dissolved in dichloromethane was used as internal standard. The procedure consisted of a pyrolysis step at 600 °C with an interface at 280 °C. The temperature in the GC-oven was first set to 40 °C and the column heated for 2.5 min, then the temperature was increased gradually (10.5 °C min^{-1}) to reach a final temperature of 300 °C for 5 min. The mass spectrometer was run in EI positive mode (70 eV; *m/z* range: 35–500, scan time: 0.204 s), and the transfer line and ion source were maintained at 250 °C and 200 °C, respectively. Blank control was conducted between every sample. Quantification was done using an external calibration curve generated for the selected indicator compound, 4-vinylcyclohexene. Which indicators to use for quantification of tyre tread material is debated (Rødland et al., 2023). Initial studies in our lab had shown that 4-vinylcyclohexene was an appropriate marker for the mix of cryo-milled car and truck tyre tread used to establish an external calibration curve. This marker has also been used by several other studies to quantify car tyre material (More et al., 2023; Mun et al., 2022). The tread material was sourced from Denmark and Sweden (Genan, Denmark), i.e., following the suggestion of Miller et al.

(2022) that regionally representative tyre tread mixes should be used to interpret the pyrograms.

2.5. Equivalent diameter (D_{eq})

The equivalent diameter (D_{eq}) of each particle was calculated according to Wadell (1932), using each particle's three side lengths A, B, and C (Eq. (1)). The particle's major and minor dimensions were obtained from the siMPle software while the third dimension was estimated as 60 % of the minor dimension as described by Simon et al. (2018) and later modified by Liu et al., (2019a). The D_{eq} was then calculated by assuming a sphere of the same volume as the ellipsoid (Eq. (1)).

$$D_{eq} = \sqrt[3]{ABC}$$

2.6. QA/QC

Several measures were taken to reduce the procedural contamination. All labware were flushed thrice with particle-free water while all filters were muffled at 500 °C prior to use. Cotton lab coats were always worn in the lab. Samples were always handled inside a fume hood and covered with aluminium foils or glass watches. All solutions were pre-filtered on 0.7 μm glass fibre filters. In addition, an air filtering device with HEPA filter (H14, 7.5 m^2) was continuously filtering the air in the lab. However, due to the pervasive presence of MPs, some contamination is inevitable. Hence, triplicate laboratory procedural blanks were prepared using washed sand (75–1000 μm, Baskarp Sand No. 15) muffled at 500 °C alongside the lake samples (Molazadeh et al., 2023). The blank control samples went through the same processes as the sediment samples. The lower size detection limit for MPs was considered as 11 μm, given that particles comprising just 1 pixel (5.5 μm) were excluded from the data analysis using siMPle, and the filter mesh size used in sample preparation was 10 μm.

The sample preparation may cause some loss of MP due to incomplete separation during, for instance, density separation. The extraction efficiency of the applied extraction protocol was assessed in a separate method study for the Danish EPA (Liu et al., 2023), which ran parallel to the current study. Here a recovery test was conducted by adding a known number of easily distinguishable plastic beads to muddy marine sediments, which then underwent the previously described sample preparation process. Four types of beads (polypropylene (PP) 45–63 and 75–90 μm; polystyrene (PS) 45–63 and 90–106 μm, Cospheric) were spiked to 24 subsamples, 6 from each of the 4 natural sediments. The MPs used for the spiking represent the most abundant environmental MPs in terms of polymer density and size, as detected by the applied protocol (Molazadeh et al., 2023). The microbeads were manually counted under a stereomicroscope (ZEISS, SteREO Discovery.V8) before being spiked to the sediment (Fig. S1). After extraction, the recovery rate was determined by counting the microbeads in the extracted aliquots, yielding average recovery rates between 50 and 90 %, mainly depending on the sediment type.

Some natural materials have spectra quite close to those of PP and polyethylene (PE). To prevent false positive identifications, these spectra were incorporated into the siMPle library as natural materials, categorised under a group named 'fake particles' (Molazade et al., 2023).

2.6 . Statistical analysis

The Shapiro-Wilk normality test was applied to assess the normality of datasets. To investigate if there were significant differences in MP sizes and mass between samples, a non-parametric Kruskal-Wallis test was performed. If differences existed, a Wilcoxon rank sum test was used for pairwise comparison. Moreover, the test was also performed on particle size comparing buoyant and non-buoyant polymers.

3. Result and discussion

3.1. Overall MP and TWP abundance

3.1.1. MP concentrations excluding TWP

Regarding MPs that could be identified by μFTIR imaging, i.e., excluding TWP, which is discussed in section 3.1.2, Brabrand Lake sediments held quite many MPs, with a global average of 11,312 count kg^{-1}, corresponding to an estimated mass of 260 mg kg^{-1} (dry weight, Table S1). The blank contamination was low compared to the measured concentrations, namely 167 item kg^{-1} and 11.99 μg kg^{-1}, corresponding to 1.48 % and 0.00546 % of the average MP number and mass concentration, respectively (for details see supplementary materials, the section on MPs in blanks). The results were not corrected for recovery as MP is a diverse group of materials, and it is debatable if measured MP concentrations should be corrected based on recovery deducted from 'ideal' particles such as microbeads.

Fig. 2 compares the MP level in Brabrand Lake sediment with other solid matrices. These data all originate from the same lab as the present study and were prepared by quite similar procedures and analysed by the same μFTIR instrument. The main reason for choosing these datasets was that comparing data analysed the same way should be less prone to quantification bias than comparing datasets across laboratories. TWP could not be included in the comparison as those studies did not report this parameter.

The lake sediment held on average 22 times more MP mass than those of sediment from a stormwater pond discharging directly to it (Molazadeh et al., 2022). However, the MP mass concentration in the lake was lower than that of a stormwater pond in another Danish city, studied by Olsen et al. (2019) (402 mg kg^{-1}). The lake sediment was on the other hand much more polluted than sediment from a Danish fjord. It held 55 times more MP than what was found in marine sediment from Odense Fjord, Denmark (Liu et al., 2021a). Comparing to a completely different matrix, namely sewage sludge, the lake sediment was slightly more polluted than sludge from a Swedish WWTP (230 mg kg^{-1}) but less polluted than digested sludge from the same plant (370 mg kg^{-1}) (Chand et al., 2021). Comparing to another type of matrix, namely the dust that accumulates on roads, the lake sediment was on average 2 times more polluted than that of road dust collected in an industrial area (Rasmussen et al., 2023). All data were compared on a dry matter basis (Fig. 2A). Comparing the number of detected MPs in the Brabrand Lake, i.e., the MP counts instead of the mass, to those other matrices, the pollution level was significantly lower than other urban matrices but in the range of the marine sediment (Odense Fjord) (Fig. 2B).

Most MPs have in literature been reported as particle counts and not mass. Compared to other lakes in different continents, our findings showed a significantly higher MP count concentration in sediment (Bharath et al., 2020; Yin et al., 2020; Gopinath et al., 2020a; Li et al., 2019; Qin et al., 2019; Dean et al., 2018; Merga et al., 2020). For instance, 396 count kg^{-1} was reported in sediment of Lake Vesijarvi in Finland (Scopetani et al., 2019). That in sediment of Lake Michigan in North America ranged from 33 to 6229 count kg^{-1} (Lenaker et al., 2019). Some of the most polluted lake sediment reported was from Lake Bizerte in Tunisia with 7960 count kg^{-1}, high but still 1.4 times below the present study (Abidli et al., 2017). However, Tangxun Lake in China (Shi et al., 2022) held on average 1.6 times more MP than Brabrand Lake, with $1.81 \pm 1.75 \times 10^4$ count kg^{-1}.

Several factors are likely to have contributed to the differences between studies: for example, true differences in concentrations at the locations, differences in sampling strategy, and differences in analytical approach. The latter is known to affect the results quite significantly, for example when analytical methods have different lower-size quantification limits and differences in analytical accuracy, making comparison across studies quite challenging (Primpke et al., 2020a,b). Moreover, the size range investigated in different studies can affect the comparison. In the current study, MPs in the range of 10–5000 μm were investigated

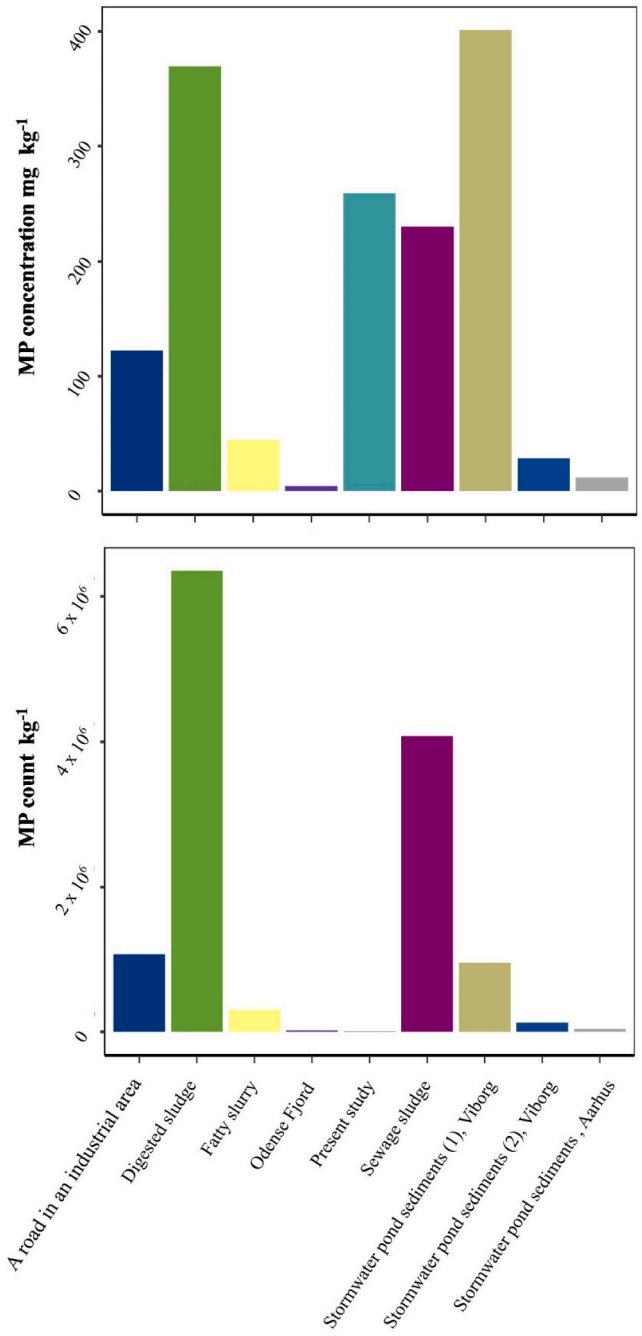

Fig. 2. MP contents reported by authors from the same lab measured in different solid matrices in terms of estimated mass (A) and count (B) per kg of dry matter. The figure only shows those MPs that could be identified by μFTIR imaging and TWP is hence not included in the datasets.

(Fig. 3). Small-sized particles tended to be more abundant, and most MPs (63 %) were smaller than 100 μm. In contrast, MPs > 400 μm accounted for only a small portion of the MPs, namely 3.5 % of all counts. Compared to for example the findings of Bharath et al., 2020 who investigated MPs > 300 μm and reported that the majority (47 %) were in the size range 300–1000 μm, in the current work only 6.6 % were in this size range and 93 % were smaller than the 300 μm which was Bharath et al.'s lower limit. In the study conducted by Lenaker et al. (2019) in Lake Michigan, MPs of their smallest size fraction (125–355 μm) made up 62 % of the MPs, while such MPs in the current study only made up around 20 %. We would have found roughly 70 % less MPs had we only studied particles > 125 μm. Lenaker et al. reported that

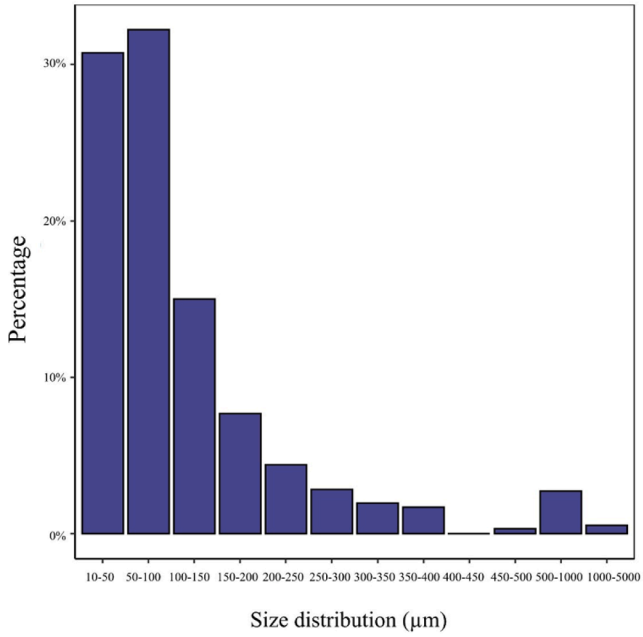

Fig. 3. Percentage of MP by counts after sorting MPs into bins according to their major dimension.

355–999 μm MPs made up 24 % of all MPs, while this size range in our study contributed only about 5 %. Shi et al. (2022) found that particles < 1000 μm were dominant in the sediments of Tangxun Lake in China when studying MPs to sizes below 50 μm (no lower size limit was stated). The same was concluded in the current study where 99.5 % of MPs were < 1000 μm.

There are several potential input pathways and sources to the lake. MPs could come via Aarhus River; however, the river passes an artificial wetland established in 1998, 3 years after the lake was dredged, and it seems reasonable to assume that much pollution would be retained here (Ziajahromi et al., 2020). Urban runoff from combined sewer overflows and separate stormwater outlets combined with outflow from the WWTP seems more likely to be significant sources (Ballent et al., 2016). Furthermore, separate stormwater can hold misconnected wastewater which then is discharged to the lake (Panasiuk et al., 2015). Diffuse sources may also play a role, as wind can carry MPs from the city and into the lake, and natural surface runoff via small streams and channels can convey MPs to the lake (Wang et al., 2022). Last but not least, MPs generated from the fragmentation of larger plastic litter cannot be excluded as a source (Lechner and Ramler, 2015).

3.1.2. *Occurrence of TWP in the lake*

The global average concentration of TWP over the lake was 19 mg kg^{-1} (Table S1). The TWP concentration of the present study can be compared to those from other laboratories, mainly because Py-GC/MS is not affected by the lower size limitation, for which data are reported in section 3.1.2. However, few such data exist for urban lakes. Hence compared to other environments, the lake was on average 264 times more polluted than the most polluted sediment sampled from the southern German Bight, and river Weser, Northwest Germany (0.072 mg kg^{-1}) (Goßmann et al., 2021). The authors measured TWP in 10 sediment samples (3 from the southern German Bight, 7 from river Weser) and reported that only 6 showed tyre wear indicator signals. It is worth noticing that the river sediments containing TWP were taken in close vicinity to a highway or city. The sediments obtained from the German Bight were collected at locations that were further away from the coastline (Goßmann et al., 2021). The TWP concentration in Brabrand Lake was lower than that of dust from a parking lot located in a commercial area and a road in an industrial area, holding respectively

69 and 2868 mg kg^{-1} TWP (Rasmussen et al., 2023). The average concentration of tyre and road wear particles (TRWP) in sediment samples from the river Seine (France), Chesapeake Bay (U.S.), and Yodo-Lake Biwa (Japan) watersheds were respectively 4500, 910 and 770 mg kg^{-1} (Unice et al., 2013). This is higher than in the present study, but to exactly what degree is not clear since Unice et al. analysed styrene butadiene rubber plus natural rubber based on styrene as marker compound and from this estimated the amount of TRWP, while the present study applied 4-vinylcyclohexene as a quantification compound for TWP by means of an external calibration curve made by a mixture of regionally sourced tyre particles. Firstly, TRWP differs from TWP by also including material from the road and its dust. Secondly, 4-vinylcyclohexene is a more specific marker for styrene butadiene rubber and butadiene rubber than styrene (Goßmann et al., 2021) but does not mark natural rubber. Direct comparison between these numbers is hence somewhat problematic.

In a modelling study conducted by Unice et al. (2019) the authors projected that 49 % of total TWP emissions go to runoff, thus runoff is a significant source of TWP to downstream systems if it doesn't receive proper treatment. Runoff from various point discharges to Brabrand Lake could hence be an important source of this pollutant in the lake.

3.2. Spatial distribution of MP

3.2.1. Mps excluding TWP

While MPs were found at all 13 locations across the lake, the spatial variation was substantial (Fig. 4). No clear trend was seen as high and low MP-concentrations seemed randomly spread across the lake. The highest abundance by counts was at L12 (38,460 counts kg^{-1}), the easternmost sampling location close to the lake outlet, while the lowest was at L1 (747 counts kg^{-1}), the westernmost sampling location where Aarhus River discharges to the lake (Table S1 and Fig. 4A). However, just south of L1 there was L2, which held 15 times more MP counts. When measured by estimated particle mass, the variation was even larger. L1 was again the least polluted location with a rather low concentration of 0.042 mg kg^{-1}. For MP mass, the highest concentration was, however found in the lake's middle region L8 (2,701 mg kg^{-1}), which was 6 orders of magnitude above L1. The variability in estimated mass was much higher than the variability in counts, which was caused by a few large MPs. For identical particle shapes, the mass comes in the third power of its dimension, and finding some large MPs hence results in a much larger estimated mass. In a study of one the stormwater ponds discharging to Brabrand Lake, Molazade et al. (2022) found a quite similar variability in the pond. Similarly, Liu et al. (2022) and Gopinath et al., (2020b) found great spatial variability for Chaohu Lake and Red Hills Lake.

When the purpose of a sampling campaign is monitoring a MP contamination level in aquatic sediments, spatial variability must hence be considered. Basing a conclusion on one or just a few grab samples is likely to yield unreliable results, either over- or underestimating the contamination level. To account for the patchiness, a quite large sampling campaign must be designed. Even the rather decent campaign of the current study was on the low side of what is recommendable if the goal is to estimate the total amount of MPs in Brabrand Lake.

The reasons for the patchiness can only be speculated on. There are probably many factors that interact and contribute to the observed variability, among which the closeness to a source can be one. It could for example be argued for L1 that it is dominated by the water from Aarhus River, which was 'pretreated' in the artificial wetland, and hence maybe low on MP. Or maybe the 'water jet' from the river flushes light particles like MPs further into the lake. Local hydraulic conditions may also explain other high or low concentrations. Maybe L2 is in a

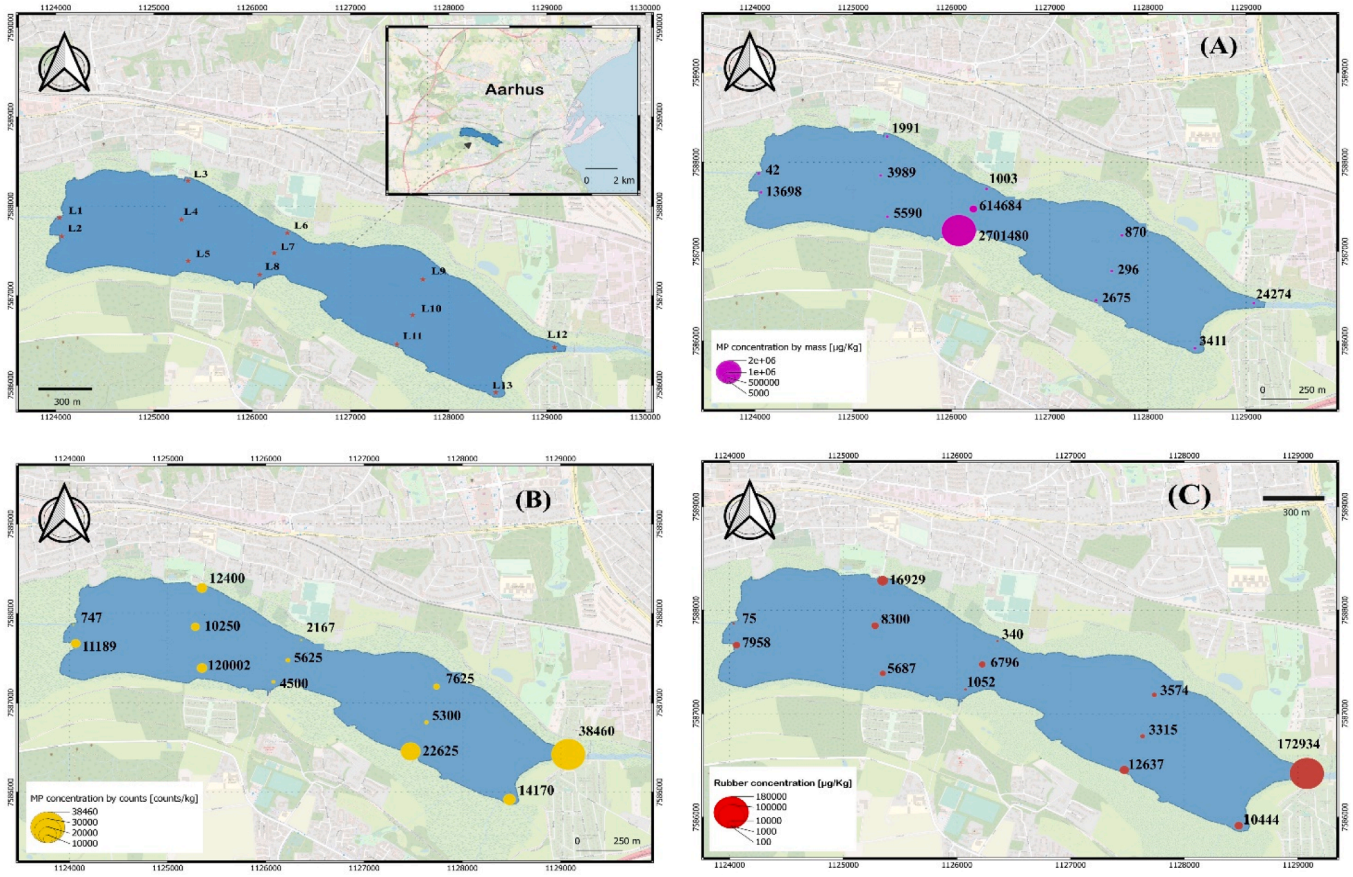

Fig. 4. Spatial distribution of MP mass (A) and counts (B) identified by µFTIR and TWP (C) over the lake.

deposition zone, leading to light particles settling out. Maybe it is protected from the predominant westerly wind. Leads et al. (2023) reported for example, that wind direction on the day of sampling was the greatest contributing factor to the MP abundance they found. However, without very detailed studies – and maybe even then – it seems unachievable to establish causality between observations and influencing factors in a system which is as dynamic as a shallow urban lake. From a pragmatic viewpoint, the patchiness might instead be treated as random.

3.2.2. Tyre wear particles

Like other MPs, the spatial distribution of settled tyre particles seemed random, and no preferential pattern could be identified (Fig. 4C). The concentration of TWP at the outlet of the lake (L12) was one order of magnitude above the highest concentration in the rest of it. L12 also held the highest MP count of other plastic types, while it in terms of mass of those MPs ranked as the third most polluted location. TWP was present in lowest concentrations at L1, which also was the least polluted in terms of other plastic types. In general, there was, however no correlation between the mass of TWP and the mass of other MP types at a location. With the caveat that it may be problematic to compare mass estimated by μFTIR and mass determined by Py-GC/MS, TWP was a minor contributor to the total MP mass at 2 of the locations (Table S1). In other cases, it was present in concentrations roughly corresponding to (3 sampling locations), or above (8 sampling locations), the sum of other plastic types (Table S1), illustrating that when assessing the MP contamination of this lake, contamination caused by tyre particles should not be overlooked.

3.3. Polymer composition, size, and mass

3.3.1. Polymer composition

In addition to tyre wear material identified by Py-GC/MS, a total of 15 polymer types were identified by μFTIR. Of those, 5 were present in rather low concentrations and were lumped into a group called 'Others' (see supplementary information for the polymer types, Table S2). They accounted for 0.15 % of the particle mass estimated by μFTIR, and 4.2 % of the particle counts. The dominant polymers as particle mass and as found by μFTIR were PP (78.7 %), PVC (10.7 %) and polyester (5 %), together constituting 94.5 % of all MPs (Fig. 5). The high composition of PP held true also when measured as particle number (34 %), now followed by polyester (23 %) and PE (15 %). The prevalence of PP in sediments of freshwater systems have been reported by other authors, for example Olesen et al. (2019), Liu et al. (2019b), Bharath et al. (2020), and Molazadeh et al. (2022). The high level of PP is probably linked to its high consumption in daily life (plastic Europe 2020). Including TWP in the analysis, the ranking changed as tyre wear particles stood as the second most abundant polymer across the lake, constituting 6.9 % of the total MPs identified. Such comparison must though be taken with a grain of salt, as comparing concentration data using different analytical approaches is not always reliable. So did Primpke et al. (2020c) find that when estimating mass from μFTIR data, the polymer masses were overestimated in samples containing larger and many particles. Doing a quite similar comparison, Kirstein et al. (2021) on the other hand found that masses correlated well when concentrations were high, but poorly when they were low.

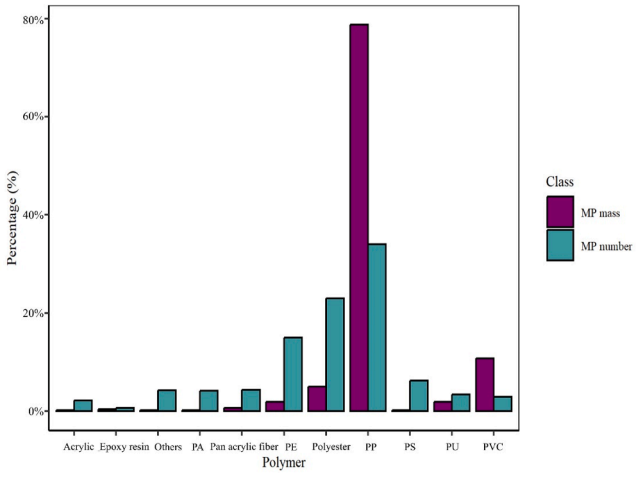

Fig. 5. Polymer composition of the MPs detected in the lake by μFTIR. The concentration is given as particle counts and estimated mass. The tyre wear particles were excluded in this graph since their number cannot be identified by Py-GC/MS.

No preferential spatial distribution of polymer composition was seen in the lake, indicating a rather random distribution. This held true for particle counts and mass (Fig. 6). Of MPs detected by μFTIR, buoyant polymers (PP + PE) were abundant at most sampling locations. Considering that PP and PE are lighter than water, there must be some process or processes causing MPs that intrinsically float to reach the sediments of the lake. This could, for instance, be mixing induced by turbulence, aggregation with microorganisms and naturally occurring particles, biofouling, and mineral formation (Lobelle and Cunliffe, 2011, Semcesen and Wells, 2021, Molazadeh et al., 2022). What is the dominant process remains speculation but considering that the average hydraulic residence time in the lake is only 12 days, and that the lake is only around a meter deep and not stratified, physical turbulence-driven transport seems a likely candidate for being the dominant mechanism (Molazadeh et al., 2022). Considering TWP, it dominated the polymer type of most sampling locations (Table S1 and S2), however, due to the limitation of Py-GC/MS to detect the number of particles, this polymer is not included in Fig. 6.

3.3.2. MP size and mass

Accounting for the size of MPs at each location, most were smaller than 100 μm (Table S2). In order to compare the size and mass distribution of MPs of different sampling locations, a non-parametric Kruskal-Wallis test (as data were not normally distributed as tested by a Shapiro-Wilk normality test) was performed (Table S4 and S5 and Fig. S2). No spatial pattern was seen for the particle size and particle mass distributions of MPs, and mass and size distribution of MPs in many, but not all, locations were similar ($p > 0.05$). This led to the conclusion that preferential accumulation of heavy and large particles had not occurred.

Despite the absence of any trends, there were some locations that showed different size and mass distribution ($p < 0.05$), which probably was due to random deposition patterns. In other words, closeness to potential sources such as the upstream wetland, the combined sewer overflows and stormwater outfalls on the northern shore, and the WWTP discharge at the southeast part of the lake did not affect the MP size and mass at the sampling locations.

3.3. The effect of MP size on MP abundance and distribution pattern

The occurrence of buoyant and non-buoyant MPs in the bed sediments at high concentration but with no obvious pattern of distribution, brough up the question how they spread across the lake. One reason for not seeing a pattern might be turbulence induced by wind and inflows, that causes eddies, which then mix the water (Bentzen et al., 2009). Small particles will follow the eddies as their intrinsic sinking or rising velocities are much smaller than the local water velocity inside the eddy (Shamskhany and Karimpour, 2022). Even dense sub-millimetre particles do not sink along a straight path but move chaotically depending on time and space-dependent flow-patterns (Molazadeh et al., 2023). Another reason could be that MPs in sediments reflect long-term accumulation. The lake is quite shallow, and strong winds can cause sediments to resuspend and redeposit. How and where will depend on parameters such as wind direction and strength. Such reshuffling of the sediments could easily mask an intrinsic pattern caused by closeness to

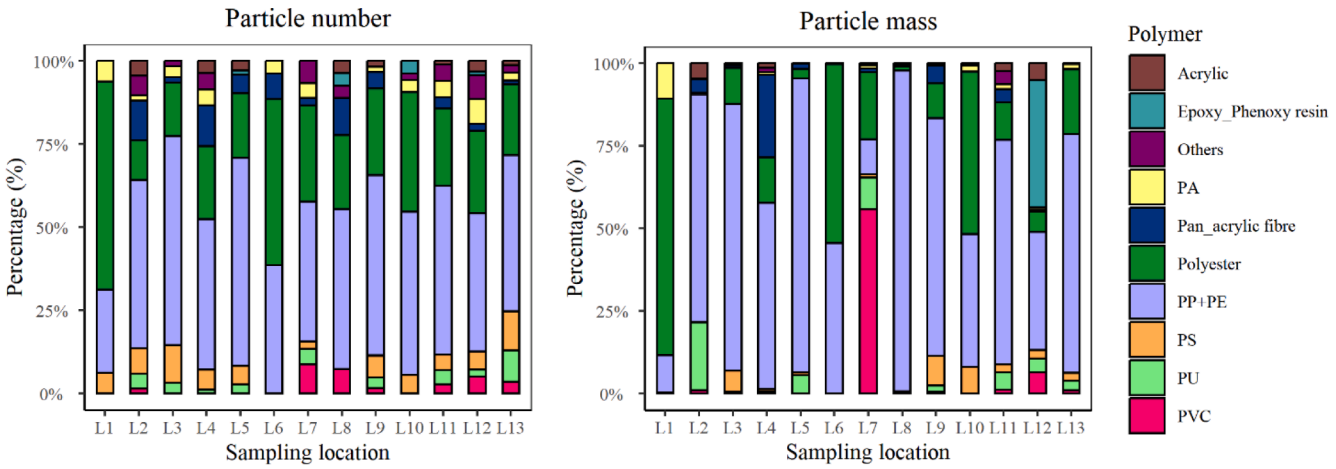

Fig. 6. Polymer composition of the MPs identified by μFTIR at each sampling locations, measured by particle counts (A) and mass (B).

sources. Moreover, from sediment transport theory it is well-known that size can play an important role in transport and sinking of particles (Shamskhani and Karimpour, 2022). For instance, regardless of their high density, small particles like silt (0.004–0.062 mm) and sand (0.06–2 mm) can be transported over long distances before reaching a low-velocity zone and settle (Shamskhani et al., 2021).

The equivalent spherical diameter (D_{eq}), which to some degree also covers the effect of shape, was applied to see if particle size had impacted the occurrence of polymers, both buoyant and non-buoyant ones (excluding tyre wear particles) (Fig. 7A and Table S6). The first question was whether particles which intrinsically should float behaved differently than particles which should intrinsically sink, i.e., buoyant versus non-buoyant MPs. A Wilcox test showed no significant difference ($p > 0.05$) between the size of buoyant and non-buoyant polymers after lumping all the MPs identified from the lake (Fig. 7A). When the test was done per sampling location, again, no significant difference was found, i.e., the size of buoyant and non-buoyant polymers was similar ($p > 0.05$). The only exception was *L*10 ($p < 0.05$).

This implies that it probably was similar processes that brought MPs to the sediment, regardless of their density. It is worth noting that 90 % of the detected particles had a D_{eq} below 250 μm. Such small particles can get entrained by flow regardless of their density, and thus behave in a similar manner (Shamskhani and Karimpour, 2022). For such small sizes, MPs' vertical motion is mainly dominated by turbulent dispersion, and the density has a minimal effect on their dispersal. This was also concluded by the modelling study of Shamskhani and Karimpour (2022), who observed that the motion of fine MPs is mainly governed by the ambient turbulent flow, while large particles' vertical motion may be dominated by gravitational settling or rising. Depending on the energy of flow, particles of different sizes and densities can become entrained and thus deviate from their natural sinking or floating behaviour and consequently be carried by the flow. Shamskhani and Karimpour (2022) for instance, showed that in a stream with a turbulent kinetic energy of 0.06 m^2/s^{-2}, 2 mm PE particles (ρ_p = 940 kg m^{-3}) could get entrained by the flow, hence hampering their rising to the surface.

This means that the vertical motion of MPs can be strongly influenced by mixing and their behaviour in turbulent flow similarly affected. How significant the effect is will depend on the turbulence, the density, and the size of the MP. A thought experiment can illustrate this. If density was the sole plastic property governing the transport and distribution of MPs, all land-based debris composed of sinking polymers

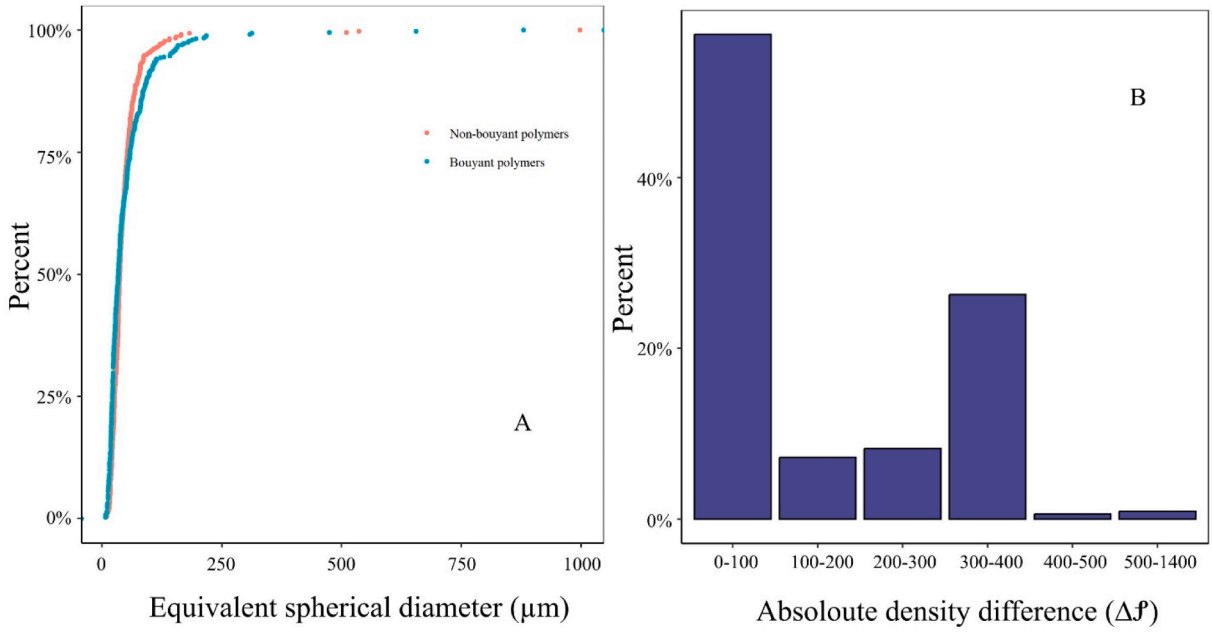

Fig. 7. Equivalent spherical diameter (D_{eq}), for buoyant and non-buoyant MPs identified by μFTIR (A) and their marginal density (B).

like PVC and PET would settle in the close vicinity of an emission source, depending on their intrinsic settling velocity in quiescent water. Moreover, low-density particles such as PE and PP would not be present in sediment and high-density polymers, such as PVC and PET ($\rho > 1.1$ g cm^{-3}), would not be found at the water surface (Liu et al., 2019a). This is obviously not the case as small particles with low marginal density ($|f_p - f_w|$) can be expected to behave like passive scalers and follow flow paths. Eddies caused by turbulence will hence occasionally cause them to encounter the sediment bed where they might get trapped. The marginal density of all MPs identified by μFTIR is shown in Fig. 7B. Most particles (57 %) had a low marginal density, i.e., within ± 10 % of that of the lake water, and 63 % of particles were < 100 μm (Fig. 7A). For fine particles, the smaller the marginal density, the more likely the particle follows the path of the flow, i.e., the streamlines. It must, though be noted that turbulent particle transport is not the only explanatory process which can contribute to explaining the observations. Small MPs have a large exterior surface area to volume ratio and their overall density would hence be more affected by biofouling and agglomeration.

3.5. Water depth and pedologic characteristics

Neither MP content identified by μFTIR nor TWP correlated to the water depth at the sampling locations. It must though be kept in mind that the water depth varied little, namely only from 0.5 to 1.5 m (Table S7). Gholizadeh and Cera (2022) also studied MPs in sediments at low water depth without finding a correlation to water depth. For a deeper lake, Cera et al. (2022) on the other hand found that deeper stations were more contaminated.

A rather weak positive correlation was found between the abundance of MPs measured as counts and the organic matter content of the sediments (Table S7) ($r^2 = 0.59$) and silt content ($r^2 = 0.47$), and there was only a rather weak or no correlation between MP concentration measured as mass and sediment properties (Fig. S3). This held true both for MPs identified by μFTIR and for TWP. Similarly, Hengstmann et al. (2018), Renzi et al. (2018) and Vermaire et al. (2017) did not observe a correlation between MP abundance and organic matter of the sediments they studied. In disagreement herewith, several other studies found that there was a positive correlation between sediment organic matter content and MP concentration (Molazadeh et al., 2022; Liu et al., 2021b; Corcoran et al., 2020). In terms of the effect of sediment grain size on MP occurrence, Alamor et al. (2016) and Laju et al. (2022) did not observe a clear trend between sediment grain size and MP deposition in coastal shallow sediments whereas Falahudin et al. (2020) and Liu et al., (2021a), Liu et al., (2021b) found that MP correlated positively with the silt content of marine and river sediments, respectively.

Conclusions on whether MP abundance varies with sediment characteristics are hence vastly diverging, indicating that other factors and environmental conditions might play a significant role on how MPs distribute in the sediments of a water body. According to our findings, the distribution of MPs in the lake sediments could be treated as random, as no parameter could predict its accumulation. The reason can be site-specific hydrodynamics of this shallow lake, in which sediment and MPs contained herein occasionally are resuspended due to waves and inflow, redistributed, and redeposited, leading to a chaotic and random distribution pattern.

4. Conclusion

High concentrations of MPs, identified by μFTIR and Py-GC/MS, were detected in the sediments of a Danish urban lake. The average level of MPs other than TWP exceeded that of sewage sludge, suggesting that the lake sediments had served as a long-term sink of plastic. The spatial variability in MP mass estimated by μFTIR imaging was up to 6 orders of magnitude, while TWP measured by Py-GC/MS varied up to 5 orders of magnitude. There was no spatial pattern in the MP distribution, indicating that a fine sampling grid is needed to accurately reflect MP abundance and distribution in such lake. PP was the most abundant polymer found in the sediments, followed by TWP, emphasising the importance of considering TWP when assessing MP contamination. The study also showed that buoyant and non-buoyant MPs shared similar distribution and were of similar size, suggesting that the same process governed their transport to the sediments.

Declaration of Competing Interest

The authors declare that they have no known competing financial interests or personal relationships that could have appeared to influence the work reported in this paper.

Data availability

Data will be made available on request.

Acknowledgements

This work was carried out within the Limnoplast project. This work was supported by European Union's Horizon 2020 research and innovation programme [860720].

Appendix A. Supplementary data

Supplementary data to this article can be found online at https://doi.org/10.1016/j.envint.2023.108282.

References

Abidli, S., Toumi, H., Lahbib, Y., Trigui El Menif, N., 2017. The first evaluation of microplastics in sediments from the complex lagoon-channel of Bizerte (northern Tunisia). Water, Air, Soil Pollution. 228, 1–10. https://doi.org/10.1007/s11270-017-3439-9.

ASTM, 2000. Standard test methods for moisture, ash, and organic matter of peat and other organic soils. Method D 2974-00. American Society for Testing and Materials, West Conshohocken, PA 2000. American Society for Testing and Materials.

Ballent, A., Corcoran, P.L., Madden, O., Helm, P.A., Longstaffe, F.J., 2016. Sources and sinks of microplastics in Canadian Lake Ontario nearshore, tributary and beach sediments. Mar. Pollut. Bull. 110, 383–395. https://doi.org/10.1016/j.marpolbul.2016.06.037.

Bentzen, T.R., Larsen, T., Rasmussen, M.R., 2009. Predictions of Resuspension of Highway Detention Pond Deposits in Interrain Event Periods due to Wind-Induced Currents and Waves. J. Environ. Eng. 135, 12. https://doi.org/10.1061/(ASCE)EE.1943-7870.0000108.

Besseling, E., Hasselerharm, P.R., Foekema, E.M., Koelmans, A.A., 2019. Quantifying ecological risks of aquatic micro- and nanoplastic. Crit. Rev. Environ. Sci. Technol. 49, 32–80. https://doi.org/10.1080/10643389.2018.1531688.

Bharath, K., M., Srinivasalu, S., Natesan, U., Ayyamperumal, R., Kalam, S.N., Anbalagan, S., Sujatha, K., Alagarasan, C.,, 2021. Microplastics as an emerging threat to the freshwater ecosystems of Veeranam lake in south India: A multidimensional approach. Chemosphere. 264. Part 2, 0045–6535. https://doi.org/10.1016/j.chemosphere.2020.128502.

Cera, A., Pierdomenico, M., Sodo, A., Scalici, M., 2022. Spatial distribution of microplastics in volcanic lake water and sediments: Relationships with depth and sediment grain size. Sci. Total Environ. 829, 0048–9697. https://doi.org/10.1016/j.scitotenv.2022.154659.

Chand, R., Kohansal, K., Toor, S., Pedersen, T.H., Vollertsen, J., 2022. Microplastics degradation through hydrothermal liquefaction of wastewater treatment sludge. Journal of Clean Production. 335, 130383 https://doi.org/10.1016/j.jclepro.2022.130383.

Cole, M., Lindeque, P., Halsband, C., Galloway, T.S., 2011. Microplastics as contaminants in the marine environment: a review. Mar. Pollut. Bull. 62, 2588–2597. https://doi.org/10.1016/j.marpolbul.2011.09.025.

Cole, M., Lindeque, P., Fileman, E., Halsband, C., Galloway, T.S., 2015. The Impact of Polystyrene Microplastics on Feeding, Function and Fecundity in the Marine Copepod Calanus helgolandicus. Environ. Sci. Tech. 49 (2), 1130–1137. https://doi.org/10.1021/es504525u.

Corcoran, P.L., 2020. Degradation of Microplastics in the Environment. Handbook of Microplastics in the Environment. https://doi.org/10.1007/978-3-030-10618-8_10-1.

Corcoran, P.L., Belontz, S.L., Ryan, K., Walzak, M.J., 2020. Factors controlling the distribution of microplastic particles in benthic sediment of the Thames River. Canada. Environmental Science & Technology. 54 (2), 818–825. https://doi.org/10.1021/acs.est.9b04896.

Dean, B.Y., Corcoran, P.L., Helm, P.A., 2018. Factors influencing microplastic abundances in nearshore, tributary and beach sediments along the Ontario shoreline

of Lake Erie. J. Great Lakes Res. 44, 1002–1009. https://doi.org/10.1016/j.jglr.2018.07.014.
Ding, L., Mao, R.F., Guo, X., Yang, X., Zhang, Q., Yang, C., 2019. Microplastics in surface waters and sediments of the Wei River, in the northwest of China. Sci. Total Environ. 667, 427–434. https://doi.org/10.1016/j.scitotenv.2019.02.332.
Dong, X., Liu, X., Hou, Q., Wang, Z., 2023. From natural environment to animal tissues: A review of microplastics(nanoplastics) translocation and hazards studies. Sci. Total Environ. 10, 158686 https://doi.org/10.1016/j.scitotenv.2022.158686.
Eriksen, M., Mason, S., Wilson, S., Box, C., Zellers, A., Edwards, W., Farley, H., Amato, S., 2013. Microplastic pollution in the surface waters of the laurentian great lakes. Mar. Pollut. Bull. 77, 177–182. https://doi.org/10.1016/j.marpolbul.2013.10.007.
Falahudin, D., Cordova, M.R., Sun, X., Yogaswara, D., Wulandari, I., Hindarti, D., Arifin, Z., 2020. The first occurrence, spatial distribution and characteristics of microplastic particles in sediments from Banten Bay. Indonesia. Science of the Total Environment. 705, 135304 https://doi.org/10.1016/j.scitotenv.2019.135304.
Gholizadeh, M., Cera, A., 2022. Microplastic contamination in the sediments of Qarasu estuary in Gorgan Bay, south-east of Caspian Sea. Iran. Science of the Total Environment. 838, 0048–9697. https://doi.org/10.1016/j.scitotenv.2022.155913.
Gopinath, K.P., Nagarajan, V.M., Krishnan, A., Malolan, R., 2020a. A critical review on the influence of energy, environmental and economic factors on various processes used to handle and recycle plastic wastes: development of a comprehensive index. J. Clean. Prod. 274, 123031 https://doi.org/10.1016/j.jclepro.2020.123031.
Gopinath, K., Seshachalam, S., Neelavannan, K., Anburaj, V., Rachel, M., Ravi, S., Bharath, M., Achyuthan, H., 2020b. Quantification of microplastic in Red Hills Lake of Chennai city, Tamil Nadu. India. Environmental Science and Pollution Research. 27, 33297–33306. https://doi.org/10.1007/s11356-020-09622-2.
Goßmann, I., Halbach, M., Scholz-Böttcher, B.M., 2021. Car and truck tire wear particles in complex environmental samples – A quantitative comparison with “traditional” microplastic polymer mass loads. Sci. Total Environ. 773, 0048–9697. https://doi.org/10.1016/j.scitotenv.2021.145667.
Gündoğdu, S., Eroldoğan, O.T., Evliyaoğlu, E., Turchini, G.M., Wu, X.G., 2021. Fish out, plastic in: global pattern of plastics in commercial fishmeal. Aquaculture. 534, 736316. https://doi.org/10.1016/j.aquaculture.2020.736316.
Hengstmann, E., Tamminga, M., Bruch, C.M., Fischer, E.K., 2018. Microplastic in beach sediments of the Isle of Rügen (Baltic Sea) - Implementing a novel glass elutriation column. Mar. Pollut. Bull. 126, 263–274. https://doi.org/10.1016/j.marpolbul.2017.11.010.
Hengstmann, E., Weil, E., Wallbott, P., C., Tamminga, M., Fischer, E.K.,, 2021. Microplastics in lakeshore and lakebed sediments – External influences and temporal and spatial variabilities of concentrations. Environ. Res. 197, 0013–9351. https://doi.org/10.1016/j.envres.2021.111141.
Islam, T., Li, Y., Rob, M.M., Cheng, H., 2022. Microplastic pollution in Bangladesh: research and management needs. Environ. Pollut. 308, 119697 https://doi.org/10.1016/j.envpol.2022.119697.
Kelly, A., Lannuzel, D., Rodemann, T., Meiners, K.M., Auman, H.J., 2020. Microplastic contamination in east Antarctic sea ice. Mar. Pollut. Bull. 154, 111130 https://doi.org/10.1016/j.marpolbul.2020.111130.
Kirstein, I.V., Hensel, F., Gomiero, A., Iordachescu, L., Vianello, A., Wittgren, H.B., Vollertsen, J., 2021. Drinking plastics? – Quantification and qualification of microplastics in drinking water distribution systems by μFTIR and Py-GCMS. Water Res. 188, 0043–1354. https://doi.org/10.1016/j.watres.2020.116519.
Knight, L.J., Parker-Jurd, F.N.F., Al-Sid-Cheikh, M., Thompson, R.C., 2020. Tyre wear particles: an abundant yet widely unreported microplastic? Environ Science and Pollution Research. 27, 18345–18354. https://doi.org/10.1007/s11356-020-08187-4.
Laju, R.L., Jayanthi, M., Immaculate Jeyasanta, K., Patterson, J., Asir, G.G., N., Narmatha Sathish, M., Patterson Edward, J.K., 2022. Spatial and vertical distribution of microplastics and their ecological risk in an Indian freshwater lake ecosystem. Sci. Total Environ. 820, 0048–9697. https://doi.org/10.1016/j.scitotenv.2022.153337.
Lechner, A., Ramler, D., 2015. The discharge of certain amounts of industrial microplastic from a production plant into the River Danube is permitted by the Austrian legislation. Environ. Pollut. 200, 159–160. https://doi.org/10.1016/j.envpol.2015.02.019.
Lenaker, P.L., Baldwin, A.K., Corsi, S.R., Mason, S.A., Reneau, P.C., Scott, J.W., 2019. Vertical distribution of microplastics in the water column and surficial sediment from the milwaukee river basin to Lake Michigan. Environ. Sci. Tech. 53, 12227–12237. https://doi.org/10.1021/acs.est.9b03850.
Li, L., Geng, S., Wu, C., Song, K., Sun, F., Visvanathan, C., Xie, F., Wang, Q., 2019. Microplastics contamination in different trophic state lakes along the middle and lower reaches of Yangtze River Basin. Environ. Pollut. 254, Part A, 0269–7491. https://doi.org/10.1016/j.envpol.2019.07.119.
Liu, F., Olesen, K.B., Borregaard, A.R., Vollertsen, J., 2019. Microplastics in urban and highway stormwater retention ponds. Science of the Total Environment. 671, 992–1000. https://doi.org/10. 1016/j.scitotenv.2019.03.416.
Liu, F., da Silva, V.H., Chen, Y., Lorenz, C., Simon, M., Vollertsen, J., Strand., J., 2023. R&D project regarding development of methods for sampling and analysis of microplastics in Danish waters. Report to the Danish EPA, pp. 73.
Liu, F., Vianello, A., Vollertsen, J., 2019b. Retention of microplastics in sediments of urban and highway stormwater retention ponds. Environ. Pollut. 255, 113335 https://doi.org/10.1016/j.envpol.2019.113335.
Liu, F., Lorenz, C., Vollertsen, J., 2021a. Havstrategi – Analyse af mikroplast-partikler i sedimenter (Microplastic particles in sediments from Danish waters 2018–2021). Last downloaded September 9th, 2023 from Report to the Danish EPA 64. https://www.emodnet-ingestion.eu/submissions/submissions_details.php?menu=39&tpd=1185&step_more=11_10_13_14&step=0821.
Liu, H., Sun, K., Liu, X., Yao, R., Cao, W., Zhang, L., Wang, X., 2022. Spatial and temporal distributions of microplastics and their macroscopic relationship with algal blooms in Chaohu Lake. China. Journal of Contaminant Hydrology. 248, 0169–7722. https://doi.org/10.1016/j.jconhyd.2022.104028.
Liu, Y., Zhang, J., Tang, Y., He, Y., Li, Y., You, J., Breider, F., Tao, S., Liu, W., 2021b. Effects of anthropogenic discharge and hydraulic deposition on the distribution and accumulation of microplastics in surface sediments of a typical seagoing river: the Haihe River. Journal of Hazardous Material. 404, 124180 https://doi.org/10.1016/j.jhazmat.2020.124180.
Lobelle, D., Cunliffe, M., 2011. Early microbial biofilm formation on marine plastic debris. Mar. Pollut. Bull. 62, 197–200. https://doi.org/10.1016/j.marpolbul.2010.10.013.
Lusher, A.L., O’Donnell, C., Officer, R., O’Connor, I., 2016. Microplastic interactions with North Atlantic mesopelagic fish. ICES J. Mar. Sci. 73, 1214–1225. https://doi.org/10.1093/icesjms/fsv241.
Malla-Pradhan, R., Suwunwong, T., Phoungthong, K., Joshi, T.P., Pradhan, B.L., 2022. Microplastic pollution in urban Lake Phewa, Nepal: the first report on abundance and composition in surface water of lake in different seasons. Environ. Sci. Pollut. Res. 29 (26), 39928–39936. https://doi.org/10.1007/s11356-021-18301-9.
Matamoros, V., Arias, C.A., Nguyen, L.X., Salvadó, V., Brix, H., 2012. Occurrence and behavior of emerging contaminants in surface water and a restored wetland. Chemosphere 88, 1083–1089. https://doi.org/10.1016/j.chemosphere.2012.04.048.
Mercy, F.T., Alam, A.R., Akbor, M.A., 2023. Abundance and characteristics of microplastics in major urban lakes of Dhaka. Bangladesh. Heliyon. 9, 4. https://doi.org/10.1016/j.heliyon.2023.e14587.
Merga, L.B., Redondo-Hasselerharm, P.E., Van den Brink, P.J., Koelmans, A.A., 2020. Distribution of microplastic and small macroplastic particles across four fish species and sediment in an African lake. Sci. Total Environ. 741, 0048–9697. https://doi.org/10.1016/j.scitotenv.2020.140527.
Miller, J.V., Marskrey, J.R., Chan, K., Unice, M., K.,, 2022. Pyrolysis-Gas Chromatography-Mass Spectrometry (Py-GC-MS)Quantification of Tire and Road Wear Particles (TRWP) inEnvironmental Matrices: Assessing the Importance ofMicrostructure in Instrument Calibration Protocols. Anal. Lett. 55, 1004–1016. https://doi.org/10.1080/00032719.2021.1979994.
Molazadeh, M., Liu, F., Simon-Sánchez, L., Vollersten, J., 2023. Buoyant microplastics in freshwater sediments – How do they get there? Sci. Total Environ. 860, 0048–9697. https://doi.org/10.1016/j.scitotenv.2022.160489.
Monclús, l., Smith, M.E., Ciesielski, T.M., Wagner, M., Jaspers, V.L.B., 2022. Microplastic Ingestion Induces Size-Specific Effects in Japanese Quail. Environ. Sci. Tech. 56 (22), 15902–15911. https://doi.org/10.1021/acs.est.2c03878.
More, S.L., Miller, V., J., Thornton, S.T., Chan, K., Barber, T.R., Unice, K.M., 2023. Refinement of a microfurnace pyrolysis-GC–MS method for quantification of tire and road wear particles (TRWP) in sediment and solid matrices. Sci. Total Environ. 874, 0048–9697. https://doi.org/10.1016/j.scitotenv.2023.162305.
Mun, S., Chong, H., Lee, J., Lim, Y., 2022. Characteristics of Real-World Non-Exhaust Particulates from Vehicles. Energies 16, 177. https://doi.org/10.3390/en16010177.
OECD, 2023. https://www.oecd.org/environment/plastic-pollution-is-growing-relentlessly-as-waste-management-and-recycling-fall-short.htm (accessed 18 August 2023).
Olesen, K.B., Stephansen, D.A., van Alst, N., Vollertsen, J., 2019. Microplastics in a stormwater pond. Water (Switzerland). 11, 1466. https://doi.org/10.3390/w11071466.
Panasiuk, O., Hedström, A., Marsalek, J., Ashley, R.M., Viklander, M., 2015. Contamination of stormwater by wastewater: A review of detection methods. J. Environ. Manage. 152, 241–250. https://doi.org/10.1016/j.jenvman.2015.01.050.
Primpke, S., Christiansen, S.K., Cowger, W., Frond, H.D., Deshpande, A., Fischer, M., Holland, E.B., Meynes, M., O’Donnell, B.A., Ossmann, B.E., Pittroff, M., Sarau, G., Scholz-Böttcher, B.M., Wiggin, J.K., 2020a. Critical assessment of analytical methods for the harmonised and cost-efficient analysis of microplastics. Appl. Spectrosc. 74, 1012–1047. https://doi.org/10.1177/0003702820921465.
Primpke, S., Cross, R.K., Mintenig, S.M., Simon, M., Vianello, A., Gerdts, G., Vollertsen, J., 2020b. EXPRESS: toward the systematic identification of microplastics in the environment: evaluation of a new independent software tool (siMPle) for spectroscopic analysis. Appl. Spectrosc. 74, 1127–1138. https://doi.org/10.1177/0003702820917760.
Primpke, S., Fischer, M., Lorenz, C., Gerdts, G., Scholz-Böttcher, B.M., 2020c. Comparison of pyrolysis gas chromatography/mass spectrometry and hyperspectral FTIR imaging spectroscopy for the analysis of microplastics. Anal. Bioanal. Chem. 412, 8283–8298. https://doi.org/10.1007/s00216-020-02979-w.
Qin, Y., , Z, Wang., Li, W., Chang, X., Yang, J, Yang, F., 2020. Microplastics in the sediment of Lake Ulansuhai of Yellow River Basin, China. Water Environment Research. https://doi.org/10.1002/wer.1275.
Rasmussen, L.A., Lykkemark, J., Andersen, T.R., Vollertsen, J., 2023. Permeable pavements: A possible sink for tyre wear particles and other microplastics? Sci. Total Environ. 869, 0048–9697. https://doi.org/10.1016/j.scitotenv.2023.161770.
Reimonn, G., Lu, T., Gandhi, N., Chen, W.T., 2019. Review of microplastic pollution in the environment and emerging recycling solutions. Journal of Renewable Material. 7 (18), 1251–1268. https://doi.org/10.32604/jrm.2019.0805.
Renzi, M., Blašković, A., Fastelli, P., Marcelli, M., Guerranti, C., Cannas, S., Barone, L., Massara, F., 2018. Is the microplastic selective according to the habitat? Records in Amphioxus Sands, Mäerl Bed Habitats and Cymodocea Nodosa Habitats, Marine Pollution Bulletin. 130, 179–183. https://doi.org/10.1016/j.marpolbul.2018.03.019.

Rødland, E.S., Gustafsson, M., Jaramillo-Vogel, D., Järlskog, I., Müller, K., Rauert, C., Rausch, J., Wagner, S., 2023. Analytical challenges and possibilities for the quantification of tire-road wear particles. TrAC Trends Anal. Chem. 165, 0165–9936. https://doi.org/10.1016/j.trac.2023.117121.

Scopetani, C., Chelazzi, D., Cincinelli, A., Esterhuizen-Londt, M., 2019. Assessment of microplastic pollution: occurrence and characterisation in Vesijärvi lake and Pikku Vesijärvi pond. Finland. Environmental Monitoring and Assessment. 191, 652. https://doi.org/10.1007/s10661-019-7843-z.

Semcesen, O.P., Wells, G.M., 2021. Biofilm growth on buoyant microplastics leads to changes in settling rates: implications for microplastic retention in the Great Lakes. Mar. Pollut. Bull. 170, 112573 https://doi.org/10.1016/j.marpolbul.2021.112573.

Shamskhany, A., Karimpour, S., 2022. Entrainment and vertical mixing of aquatic microplastics in turbulent flow: The coupled role of particle size and density. Mar. Pollut. Bull. 184, 0025–0326. https://doi.org/10.1016/j.marpolbul.2022.114160.

Shi, M., Li, R., Xu, A., Su, Y., Hu, T., Mao, Y., Qi, S., Xing, X., 2022. Huge quantities of microplastics are "hidden" in the sediment of China's largest urban lake—Tangxun Lake. Environ. Pollut. 307, 0269–7491. https://doi.org/10.1016/j.envpol.2022.119500.

Simon, S., Van Last, N., Vollertsen, J., 2018. Quantification of microplastic mass and removal rates at wastewater treatment plants applying Focal Plane Array (FPA)-based Fourier Transform Infrared (FT-IR) imaging. Water Res. 142, 0043–1354. https://doi.org/10.1016/j.watres.2018.05.019.

Simon-Sánchez, L., Grelaud, M., Lorenz, C., Garcia-Orellana, J., Vianello, A., Liu, F., Vollertsen, J., Ziveri, P., 2022. Can a sediment core reveal the Plastic Age? – Microplastic preservation in a coastal sedimentary record. Environ. Sci. Tech. 56, 16780–16788. https://doi.org/10.1021/acs.est.2c04264.

Søndergaard, M., Jeppesen, E., Jensen, J.P., Lauridsen, T., 2008. Lake restoration in Denmark. Lakes & Reservoirs: Science, Policy and Management for Sustainable Use. 5, 133–212. https://doi.org/10.1046/j.1440-1770.2000.00110.x.

Unice, K.M., Kreider, M.L., Panko, J.M., 2013. Comparison of tire and road wear particle concentrations in sediment for watersheds in France, Japan, and the United States by quantitative pyrolysis GC/MS analysis. Environ. Sci. Tech. 47, 8138–8147. https://doi.org/10.1021/es400871j.

Unice, K.M., Weeber, M.P., Abramson, M.M., Reid, R.C.D., Gils, J.A.G.V., Markus, A.A., Vethaak, A.D., Panko, J.M., 2019. Characterising export of land-based microplastics to the estuary - Part I: Application of integrated geospatial microplastic transport models to assess tire and road wear particles in the Seine watershed. Sci. Total Environ. 646, 1639–1649. https://doi.org/10.1016/j.scitotenv.2018.07.368.

Vermaire, J.C., Pomeroy, C., Herczegh, S.M., Haggart, O., Murphy, M., 2017. Microplastic abundance and distribution in the open water and sediment of the Ottawa River, Canada, and its tributaries. FACETS. 2, 301–314. https://doi.org/10.1139/facets-2016-0070.

Vianello, A., Jensen, R.L., Liu, L., Vollertsen, J., 2019. Simulating human exposure to indoor airborne microplastics using a Breathing Thermal Manikin. Sci. Rep. 9, 8670. https://doi.org/10.1038/s41598-019-45054-w.

Wadell, H. Volume, Shape, and Roundness of Rock Particles., 1932. J. Geol. 40, 443−451.

Wang, F., Lai, Z., Peng, G., Luo, L., Liu, K., Huang, X., Xu, Y., Shen, Q., Li, D., 2021. Microplastic abundance and distribution in a Central Asian desert. Sci. Total Environ. 800, 0048–9697. https://doi.org/10.1016/j.scitotenv.2021.149529.

Wang, C., O'Connor, D., Wang, L., Wu, W.M., Luo, J., Hou, D., 2022. Microplastics in urban runoff: Global occurrence and fate. Water Res. 225, 0043–1354. https://doi.org/10.1016/j.watres.2022.119129.

Yang, S., Zhou, M., Chen, X., Hu, L., Xu, Y., Fu, W., Li., C.,, 2022. A comparative review of microplastics in lake systems from different countries and regions. Chemosphere 286, 131806. https://doi.org/10.1016/j.chemosphere.2021.131806.

Yin, L., Wen, X., Du, C., Jiang, J., Wu, L., Zhang, Y., Hu, Z., Hu, Z., Feng, Z., Zhou, Z., Long, Y., Gu, Q., 2020. Comparison of the abundance of microplastics between rural and urban areas: A case study from East Dongting Lake. Chemosphere 244, 0045–6535. https://doi.org/10.1016/j.chemosphere.2019.125486.

Yonkos, L.T., Friedel, E.A., Perez-Reyes, A.C., Ghosal, S., Arthur, C.D., 2014. Microplastics in Four Estuarine Rivers in the Chesapeake Bay, U.S.A. Environ. Sci. Tech. 48, 24, 14195–14202. https://doi.org/10.1021/es5036317.

Ziajahromi, S., Drapper, D., Hornbuckle, A., Rintoul, L., Leusch, F.D.L., 2020. Microplastic pollution in a stormwater floating treatment wetland: detection of tyre particles in sediment. Sci. Total Environ. 713, 136356 https://doi.org/10.1016/j.scitotenv.2019.136356.

Further reading

Shamskhany, A., Li, Z., Patel, P., Karimpour, S., 2021. Evidence of microplastic size impact on mobility and transport in the marine environment: a review and synthesis of recent research. Front. Mar. Sci. 8, 1869. https://doi.org/10.3389/fmars.2021.760649.